

Effect of an unstirred layer on the membrane permeability of anandamide

Inge N. Bojesen^{1,*} and Harald S. Hansen[†]

Department of Medical Biochemistry and Genetics,* Laboratory B, University of Copenhagen, Panum Institute, DK-2200 Copenhagen N, Denmark; and Department of Pharmacology and Pharmacotherapy,[†] Danish University of Pharmaceutical Sciences, DK-2100 Copenhagen Ø, Denmark

Abstract To study the effect of an unstirred layer (UL), we have investigated the exchange efflux kinetics of anandamide at 0°C, pH 7.3, from albumin-free as well as from albumin-filled human red blood cell ghosts to media of various BSA concentrations ($[BSA]_o$). The rate constant (k_m) of unidirectional flux from the outer membrane leaflet to BSA in the medium increased with the square root of $[BSA]_o$ in accordance with the existence of a UL, which is a water layer adjacent to the membrane that is not subject to the same gross mixing that takes place in the rest of the medium. From k_m , it is possible to calculate the rate constant of anandamide dissociation from BSA (k_1) if we know the membrane binding of anandamide, the equilibrium dissociation constant of BSA-anandamide complexes, and the diffusion constant of anandamide. We estimated k_1 to be $3.33 \pm 0.27 \text{ s}^{-1}$. The net flux of [³H]anandamide is balanced by an equal and opposite movement of nonradioactive anandamide in exchange efflux experiments. This means that our results are also valid for uptake. We show that for anandamide with rapid membrane translocation, UL causes a significant resistance to cellular uptake. Depicting the rate of anandamide uptake as a function of equilibrium water phase concentrations results in a parabolic uptake dependence. Such apparent "saturation kinetics" is often interpreted as indicating the involvement of transport proteins. The validity of such an interpretation is discussed.—Bojesen, I. N., and H. S. Hansen. Effect of an unstirred layer on the membrane permeability of anandamide. *J. Lipid Res.* 2006. 47: 561–570.

Supplementary key words red blood cell membranes • erythrocyte ghosts • membrane binding • exchange efflux • rate constant of anandamide dissociation from albumin • diffusion coefficient of anandamide

Anandamide is found in mammalian tissues, where it accumulates upon tissue injury (1–3). It is also an endocannabinoid (4) that has been suggested to be involved in pain regulation (5) and as a retrograde messenger in the nervous system, where membrane passage is important for its function and disposal (6).

Hydrophilic molecules such as amino acids need membrane transporters/channels to pass through the lipophilic plasma membrane (7). Although anandamide is a neutral lipophilic molecule with low monomeric solubility in water (8), the uptake of anandamide into cells has also been suggested to be mediated by a membrane transporter (9–14). The permeation of cellular membranes has been studied in several cell types (9, 11, 12). The existence of such an anandamide transporter is an important but controversial subject that divides researchers into two groups of apparently incompatible opinions (15–20). The evidence for the existence of an anandamide transporter in the plasma membrane comes from saturable uptake kinetics in cells and from the use of inhibitors, but to date no carrier proteins have been isolated.

Studies have reported both saturable and nonsaturable uptake kinetics using total anandamide concentration as a variable (17, 20–22). However, according to conventional theory for the cellular uptake of protein-bound lipophilic compounds, only the free monomer lipophilic compound participates in the uptake process. When studying the transport of lipophilic compounds whose membrane translocation is rapid, it is important to consider the effect of an unstirred layer (UL) around cells, because it may also be a rate-limiting barrier for transport (23, 24). Therefore, finding saturable kinetics may not be a definitive proof for a carrier-mediated process.

Furthermore, intracellular metabolism by fatty acid amide hydrolase, binding to cellular proteins and binding to plastic tools in the absence of albumin, may complicate the measurement of the true membrane passage of anandamide (10, 11, 18, 25, 26). We have used red blood cell ghosts, which classically have been used for transport studies of chloride, bromide, iodide, thiocyanate, salicylate, and glucose (27–29). All of these water-soluble compounds pass the membrane by facilitated diffusion, and the studies are carried out from 0°C to 37°C. These studies

Manuscript received 16 September 2005 and in revised form 9 December 2005.

Published, JLR Papers in Press, December 19, 2005.
DOI 10.1194/jlr.M500411-JLR200

[†]To whom correspondence should be addressed.
e-mail: norby@imbq.ku.dk

Copyright © 2006 by the American Society for Biochemistry and Molecular Biology, Inc.

This article is available online at <http://www.jlr.org>

show that protein-mediated transport can be studied at low temperatures, and because the translocation of anandamide is extremely rapid, we have chosen 0°C to get reliable results. Furthermore, it is possible to study the transport process without metabolism and the involvement of ATP and by using exchange efflux without a substrate gradient.

Diffusional barriers are important when transport processes are studied. Diffusional resistance in a UL will be the dominant factor if transmembrane movement is fast, as is the case for lipophilic compounds such as anandamide. Failure to consider the effect of a UL may result in erroneous estimation of uptake rates. One of the effects of a UL is that the clearance of unbound lipophilic compound is enhanced when albumin concentration is increased. This phenomenon led to different theories, such as the existence of albumin receptors on cell surfaces and conformational changes and/or local factors at the cell surface, which cause an enhancement of the dissociation of ligand-albumin complexes (surface-mediated dissociations) (30). However, receptors for albumin have never been found, and these speculations ended, especially after the elegant study of Weisiger, Pond, and Bass (30). They studied the effect of albumin concentration on oleate fluxes in a system of decane (lipid phase) separated from a stirred water phase by an unstirred planar interface and found that a decrease in the effective diffusion barrier with increasing albumin concentration resulted in an enhancement of the flux.

Cellular uptake of anandamide occurs only when it is in the monomeric form in a sequence of at least three steps: release from its binding protein, membrane transfer, and binding by intracellular binding proteins or by enzymes (19). The release of anandamide from cells occurs by the same three steps in reverse order. It is important to understand the mechanism by which anandamide passes membranes to elucidate whether a putative membrane transporter is a pharmacological target (12, 31) or whether cellular uptake is governed only by diffusion. One strong argument for the involvement of a protein is the apparent evidence of "saturable uptake." The aim of this study was to find an alternative interpretation of the apparent saturable uptake.

MATERIALS AND METHODS

Materials

Labeled anandamide (*[N*-arachidonyl-5,6,8,9,11,12,14,15-³H]ethanolamine; 215 Ci/mmol) was obtained from Perkin-Elmer Life Sciences, Inc. (Boston, MA). Unlabeled anandamide was purchased from Biomol Research Laboratories, Inc. The purity of both anandamides was controlled by an elution pattern of a single compound in chromatography on a 160 × 0.8 mm column filled with Sephadex LH-20 using dichloromethane as eluent. [³H]inulin (5 Ci/mmol) was from Amersham Biosciences (Hillerød, Denmark). The scintillation fluid was Ultima Gold from Packard Instrument Co., Inc., and BSA fraction V (fatty acid-free) from Boehringer Mannheim GmbH.

Preparation of erythrocyte ghosts

The preparation of a uniform population of BSA-free and BSA-filled resealed "pink" ghosts from freshly drawn human blood was carried out as described previously (19, 32). The pink ghosts, which still contain ~3% hemoglobin, are very robust and qualified for transport studies. After preparation, the ghosts were stored at 0°C in 165 mM KCl, 2 mM phosphate buffer, pH 7.3, containing 0.02 mM EDTA/EGTA (1:1) (buffer I) containing BSA of appropriate concentrations and used for experiments within 2 days. The density of ghosts was 1.02 g/ml; for calculations, we use 1 g of packed ghosts, which is equal to 1 ml. Eight donors, both men and women (age 21–64 years), were used.

Preparation of incubation buffers

[³H]anandamide and unlabeled anandamide was dissolved in 50 μl of benzene, just enough to moisten 200 mg small glass beads (diameter, 0.1 mm). The benzene was sublimated at low pressure, and incubation buffers were prepared by shaking the anandamide-loaded beads with a solution of BSA in buffer I for 15 min at room temperature.

Efflux experiments with ghosts

One volume of packed ghosts (with or without internal BSA) was equilibrated with 1.5 volume of incubation buffer at 0°C for 50 min. Radioactive ghosts were separated from buffer I containing labeled as well as unlabeled anandamide by centrifugation for 7 min at 30,100 *g* and washed with 10 volumes of buffer I, pH 7.3, at 0°C. These washed suspensions of ghosts were distributed onto 80 mm plastic tubes (inner diameter, 3 mm) and packed by centrifugation for 10 min at 17,000 *g* at 0°C. The supernatant was removed by cutting the plastic tube just below the interface, and ~100–200 mg of packed ghosts was injected into 35 ml of vigorously stirred isotope-free buffer I containing BSA and unlabeled anandamide corresponding to the cellular *v* value. Serial sampling of cell-free extracellular medium was done with the Millipore-Swinnex filtration technique. Ten to 15 samples were taken at appropriate intervals for the determination of the extracellular accumulation of radioactivity as a function of time. The activity of filtrates was measured by counting 400 μl in 3.9 ml of scintillation fluid. The efflux experiments were all carried out at 0°C as with the fast efflux of anandamide from ghosts our manual sampling technique does not allow higher temperatures.

In control efflux experiments at low *v* (0.065) as well as at higher *v* (0.4) with no albumin in the outer medium, we found <3.2% of the dpm in the medium. Furthermore, no increase in dpm by time was found.

Calculation of the unknown diffusion coefficient of anandamide

To our knowledge, the diffusion coefficient of anandamide has never been measured. An approximate value can be calculated on the basis of the theory of diffusion in liquids. With the assumption that anandamide is spherical and much larger than the water molecules, we can use the Sutherland-Einstein equation

$$D = RT/6 \pi \eta r N \quad (Eq. 1)$$

where *R* is the gas constant [$8.314 \times 10^7 \text{ g cm}^{-2} \text{ s}^{-2} \text{ mol}^{-1} \text{ K}^{-1}$], *T* is temperature (K), η is the viscosity of water at 0°C (1.798 centipoise = $1.798/100 \text{ g s}^{-1} \text{ cm}^{-1}$), *r* is the radius of the spherical particle, and *N* is Avogadro's number (6.02×10^{23} molecules per mol).

Furthermore, if anandamide consists of spherical particles of radius r and density d , its molecular weight (MW) should be

$$MW = (4/3)\pi r^3 N d \quad (Eq. 2)$$

If this equation is solved for r , and the resulting expression is substituted in equation 1, it follows that

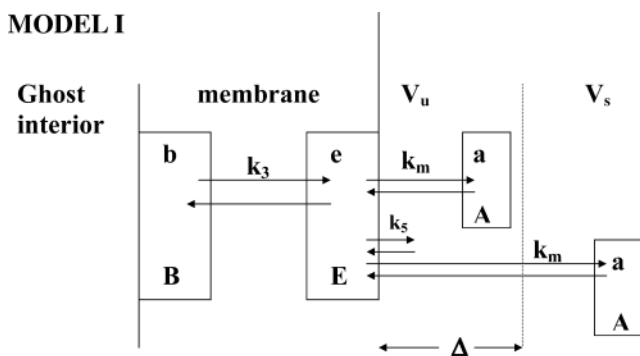
$$D = RT/(6 \pi \eta N (3MW/(4 \pi N d))^{1/3}) \quad (Eq. 3)$$

With a density $d = 0.92 \text{ g ml}^{-1}$ (Sigma-RBI Handbook of Cell Signaling and Neuroscience), we get $D = 209.5 \mu\text{m}^2 \text{ s}^{-1}$. This is the value used in equation 15. It seems to be a reasonable value because the corresponding diffusion coefficient for arachidonic acid is $310 \mu\text{m}^2 \text{ s}^{-1}$ (33) and anandamide is a larger molecule.

Theory of efflux

Efflux from BSA-free ghosts. We use the same models used in our studies of efflux of long-chain fatty acids from human red blood cell ghosts (19, 33, 34). The exchange kinetics follows a bi-exponential time course according to compartment model I shown in Fig. 1. The solution of the second order differential equation, which describes the kinetics, is according to a previous publication (19)

MODEL I



MODEL II

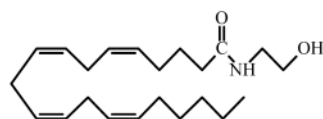
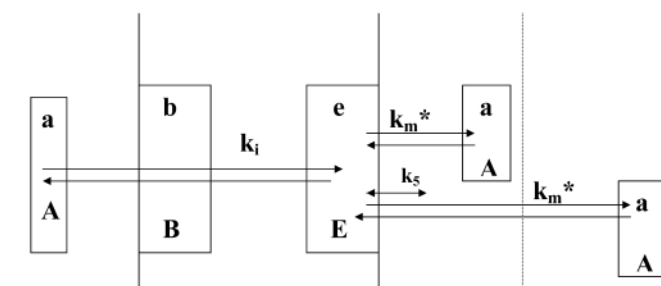


Fig. 1. The compartment models used to account for the efflux of [^3H]anandamide from ghosts in nonisotopic equilibrium with the medium. Model I: Ghosts without serum albumin. Model II: Ghosts with serum albumin. Arrows indicate unidirectional anandamide fluxes. k_3 , k_5 , k_m , k_i , and k_m^* are first order rate constants of fluxes between adjacent compartments. Lowercase letters a, b, e, and c, refer to [^3H]anandamide concentrations, and uppercase letters A, B, E, and P refer to anandamide concentrations (see Notations in Appendix).

$$1 - y/y_\infty = C1 e^{-\alpha t} + C2 e^{-\beta t}; (C1 + C2) = 1 \quad (Eq. 4)$$

and the connections between the parameters of the model [B/E , k_m , and k_3 (Fig. 1)] are

$$k_m = \alpha + \beta - \alpha\beta/(\alpha C1 + \beta C2) \quad (Eq. 5)$$

$$k_3 = \alpha \beta/k_m \quad (Eq. 6)$$

$$1 + B/E = k_m/(\alpha C1 + \beta C2) \quad (Eq. 7)$$

The efflux data were fitted to obtain maximum correlation coefficient (R) by nonlinear regression analyses using the software Origin 6 (Microsoft), and model parameters are calculated according to equations 5–7.

Efflux from BSA-filled ghosts. In model II, accounting for anandamide efflux from BSA-filled ghosts to BSA in the medium, two new rate constants are defined. k_i is the rate constant for the unidirectional anandamide flow from internal anandamide-BSA complexes to the outer surface of the ghost membrane, and k_m^* is the constant for the unidirectional flow from the membrane outer surface to BSA in the medium (19).

Again, the exchange kinetics follows a biexponential time course. The solution of the second order differential equation, which describes the kinetics, is in this case

$$1 - y/y_\infty = C3 e^{-\gamma t} + C4 e^{-\delta t} \quad (Eq. 8)$$

and the connections between the parameters of model II are now

$$k_m^* = \gamma + \delta - \gamma \delta/(\gamma C3 + \delta C4) \quad (Eq. 9)$$

$$k_i = \gamma \delta/k_m^* \quad (Eq. 10)$$

$$1 + A_i/E = k_m^*/(\gamma C3 + \delta C4) \quad (Eq. 11)$$

where A_i is the amount of anandamide bound to intracellular BSA ($[\text{BSA}]_i$).

Calculation of the rate constant for anandamide dissociation from BSA

Previously, in our studies on arachidonic acid and oleic acid, it was possible to present an expression for the determination of the dissociation rate constant from BSA (33, 34). All details are given in those two publications in Appendix A and Appendix 2, respectively. The analogous equation for anandamide becomes

$$k_1 = [(k_m C (1 - \nu)/((1 + B/E) (K_{dm} (1 - \nu) + K_d \nu)) - (1/R_D)]/S]^2 (K_d/(D (1 - \nu) [\text{BSA}]_o)) \quad (Eq. 12)$$

where C is the binding capacity of the membrane for anandamide and K_{dm} is the equilibrium constant for anandamide dissociation from the membrane. For other constants, see Appendix.

From the definition of the two dissociation constants K_d and K_{dm} , we get

$$K_d = P (1 - \nu)/\nu \text{ and } K_{dm} = P (C - M)/M \quad (Eq. 13)$$

where M is anandamide uptake by ghosts (membrane binding) in nmol g^{-1} ghosts. Eliminating the water phase monomer concentration P from the two equations gives

$$C = M [(K_{dm}/K_d) (1 - \nu) + \nu]/\nu \quad (Eq. 14)$$

Substitution of C into the equation for k_1 gives

$$k_1 = \left[\frac{(k_m M (1 - \nu) / (K_d \nu (1 + B/E))) - (1/R_D)] / S \right]^2 (K_d / (D (1 - \nu) [BSA]_o)) \quad (Eq. 15)$$

This means that k_1 can be calculated when the rate constant k_m , $[BSA]_o$, the membrane binding (M), ν , the equilibrium dissociation constant of the anandamide-BSA complex (K_d), the diffusion resistance (R_D), the area of ghosts (S), and the diffusion coefficient of anandamide (D) all are known.

Scintillation counting

We used a Tri-Carb 2200CA liquid scintillation analyzer from Packard. The efficiency is 67% for ^3H in unquenched samples using 3.9 ml of Ultima Gold scintillation fluid. Counting rates were determined to a probable error of <1%.

Statistics and data analyses

The linear and nonlinear regression procedures given by Origin 6 were used to determine the best fit of the data to the exponentials of the model. The formula to calculate the variations of terms is the general formula

$$\text{var}(T(a, b, c, \dots)) = \text{var } a (dT/da)^2 + \text{var } b (dT/db)^2 + \text{var } c (dT/dc)^2 + \dots \text{ and SD } (T) \text{ as } (\text{var}(T))^{1/2} \quad (Eq. 16)$$

RESULTS

Calculation of the dissociation rate constant for anandamide-BSA complexes

The dissociation rate constant k_1 of BSA-anandamide complexes can be calculated from equation 15 using the values of R_D , S, K_d , and D (see Notations in Appendix for values) and corresponding pairs of k_m and $[BSA]_o$ and of M and ν values. The results are given in **Table 1**.

Exchange efflux of anandamide from BSA-free ghosts

Analogous to a previous study (19), the efflux follows the expected biexponential time course. Analyses are carried out by nonlinear regression, and the integration constants C1 and C2 and the rate coefficients α and β are determined. The model parameters k_m , k_3 , and B/E (see Fig. 1

and Notations) are determined by equations 5, 6, and 7, respectively.

The most important information is that the ratio of anandamide bound to the inner leaflet to anandamide bound to the outer leaflet of ghost cell membranes (B/E) and the rate constant of unidirectional flow through the membrane from B to E (k_3) are both constant at all concentrations of BSA in the medium ($[BSA]_o$). The values are 0.27 and 0.36 s^{-1} (19), respectively. However, the rate constant (k_m) of the unidirectional flow of anandamide from the ghost membrane to BSA in the medium is dependent on $[BSA]_o$ (Table 1). This was not expected from the true exchange kinetics. This dependence, however, is understood when the effect of the UL around ghosts is taken into consideration. We have to consider the tracer uptake by BSA in unstirred volume V_u as well as in stirred volume V_s (see Appendix). For the parameters, see Notations.

As outlined in the Appendix, equation A12 is used to fit three constants (1, 2, and 3) to determine the rate constant (k_5) of anandamide dissociation from membrane binding sites to the adjacent water phase and to demonstrate the validity of the model. **Figure 2A** shows the $1/k_m$ dependence of $([BSA]_o)^{1/2}$ according to equation A12 with the three constants 1, 2, and 3 (eq. A13). Constant 2 is the most reliable of the three constant. It can be calculated from values of M, ν , R_D , and K_d using $M = 5.25 \text{ nmol g}^{-1}$, $\nu = 0.198$, $R_D = 0.022 \text{ s ml}^{-1}$, and $K_d = 6.87 \cdot 10^{-12} \text{ mol ml}^{-1}$ (see Notations), so we fixed it at the calculated value of 67.55. The fitting procedure gives a rate constant k_5 equal to $4.2 \pm 0.4 \text{ s}^{-1}$ and a constant 3 of $410,374 \pm 27,230$, which is to be compared with the calculated value of constant 3 (256,985) using $\nu = 0.198$, $k_1 = 3.33 \text{ s}^{-1}$, and the values of R_D , S, D, and K_d given in Notations. **Figure 2B** shows the $1/k_m$ dependence of $1/([BSA]_o)^{1/2}$. Here, linear regression analysis according to equation A14 gives a fit with an *R* value of 0.995 and a Chi-square value of <0.002, indicating the validity of the model.

The rate constant (k_5) is again determined to be $4.2 \pm 0.3 \text{ s}^{-1}$, and the fitted value of constant 4 is $1.6 \times 10^{-4} \pm 0.1 \times 10^{-4}$. The theoretical calculated value of constant 4 using $M = 5.25 \text{ nmol g}^{-1}$, $\nu = 0.2$, $S = 144 \times 9 \times 10^9 \times 10^{-12} \text{ cm}^2$, $k_1 = 3.33 \text{ s}^{-1}$, $K_d = 6.87 \times 10^{-12} \text{ mol ml}^{-1}$, and $D = 209.5 \text{ } \mu\text{m}^2 \text{ s}^{-1}$ turns out to be $2.6 \times 10^{-4} \pm 0.4 \times 10^{-4}$. It can only be a try, because to our knowledge the diffusion coefficient of anandamide is not available, but with the calculated $D = 209.5 \text{ } \mu\text{m}^2 \text{ s}^{-1}$ and in view of the heterogeneous population of red blood cells from very different donors (see Materials and Methods), the agreement is remarkable and thereby demonstrates the validity of our model. It is noteworthy that the rate constants of anandamide dissociation from BSA ($k_1 = 3.33 \pm 0.27 \text{ s}^{-1}$) and from the ghost membranes ($k_5 = 4.2 \pm 0.4 \text{ s}^{-1}$) are very much alike.

According to the theory, k_m should not be dependent on ν . This can be seen from equation A14. If we rewrite equation A14 as

$$1/k_m = 1/k_5 + [M ((1 - \nu)^{1/2} / \nu)] [1 / (S (D k_1 K_d)^{1/2})] [1 / ([BSA]_o)^{1/2}]$$

TABLE 1. Values of rate constant k_1 of anandamide dissociation from BSA at 0°C calculated according to equation 15

$[BSA]_o$	k_1 (a)	k_1 (b)	k_1 (c)	k_m
μM			s^{-1}	
7.5	4.22 ± 1.53	4.13	3.54	0.487 ± 0.055
15	3.40 ± 1.07	3.32	2.90	0.613 ± 0.047
30	3.52 ± 0.96	3.44	3.07	0.874 ± 0.010
60	2.92 ± 0.79	2.85	2.57	1.120 ± 0.011
Mean	3.33 ± 0.27	3.44	3.02	

k_m is the rate constant of anandamide transport from the outer surface of the ghost membrane to medium BSA (19). k_1 (a) is calculated for $M = 5.25 \pm 0.39 \text{ nmol g}^{-1}$ ghosts, $\nu = 0.198 \pm 0.018$ ($n = 9$) (19); k_1 (b) is calculated for $M = 2.53 \text{ nmol g}^{-1}$ ghosts, $\nu = 0.1$ (19); k_1 (c) is calculated for $M = 38.3 \text{ nmol g}^{-1}$ ghosts, $\nu = 0.784$ (19). The value for B/E = 0.275 ± 0.023 , and the remaining parameters are defined in Notations in the Appendix.

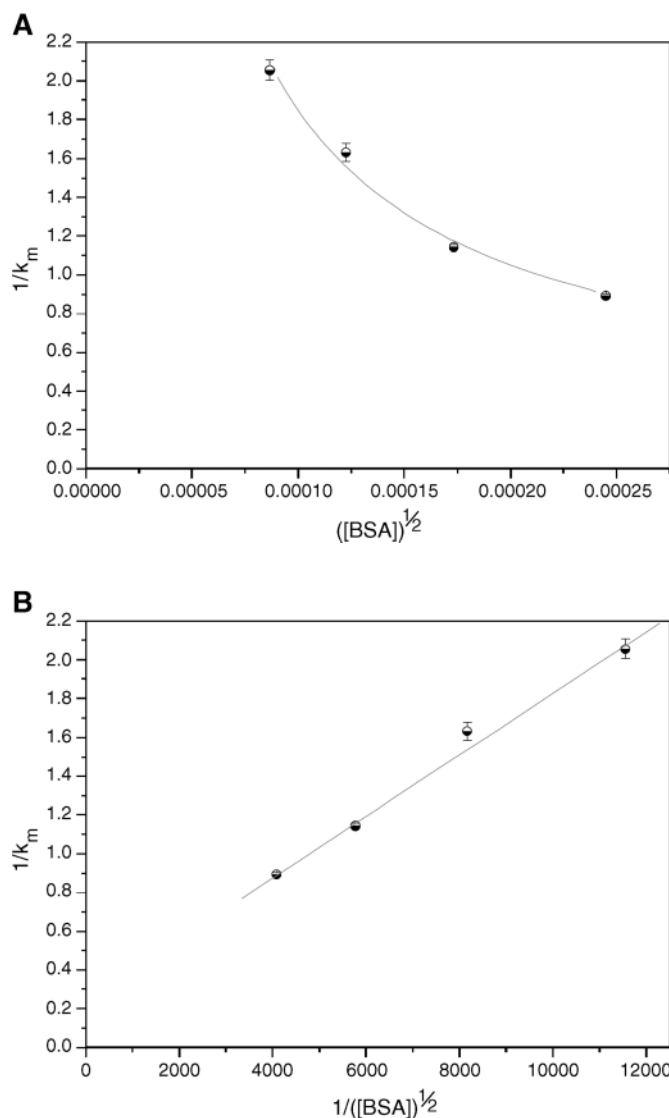


Fig. 2. A: Relationship between the reciprocal value of the rate constant (k_m) for unidirectional flow from the membrane outer surface to albumin in the medium and the square root of the albumin concentration in the medium ($[BSA]_o$). The solid curve shows the fit of data to equations A12 and A13 with three parameters. Nonlinear regression analysis gives $Y = 0.236 \pm 0.082 + 67.55 [1/(410,374 \pm 27,230 X + 1)]$. $R = 0.992$ (i.e., constant 1 = 0.236 ± 0.082 , constant 2 = 67.55, and constant 3 = $410,374 \pm 27,230$). B: The k_m dependence of $[BSA]_o$ presented according to the linearized equation A14, which is in accordance with the predicted effect of the unstirred layer (UL) around ghosts. The regression line is $Y = 1.58 \times 10^{-4} \pm 0.10 \times 10^{-4} X + 0.236 \pm 0.060$; $R = 0.995$. Error bars represent SD.

all terms except for $[M ((1 - \nu)^{1/2}/\nu)]$ are constant, and calculation of $[M ((1 - \nu)^{1/2}/\nu)]$ shows that the expression is virtually constant. For a variation in ν with a factor of >7 from 0.102 to 0.784, M varies from 2.53 to $38.34 \text{ nmol g}^{-1}$, to give a nearly constant value of the term $[M ((1 - \nu)^{1/2}/\nu)]$ as it varies from 23.50 and 22.73.

Direct experimental verification of this constancy is obtained by efflux experiments at low and high ν values. At $[BSA]_o = 15 \text{ } \mu\text{M}$, we get $k_m = 0.649 \pm 0.074 \text{ s}^{-1}$ at low ν

value (0.06) and $0.622 \pm 0.066 \text{ s}^{-1}$ at high ν value (0.4). When $[BSA]_o = 30 \text{ } \mu\text{M}$, $k_m = 0.712 \pm 0.093 \text{ s}^{-1}$ at low ν value (0.05) and $0.815 \pm 0.062 \text{ s}^{-1}$ at high ν value (0.4). These results are again weighty evidence for the validity of the model.

Exchange efflux of anandamide from BSA-filled ghosts

These kinds of experiments show that anandamide effluxes are much slower than from BSA-free ghosts (19). The experimental values for the rate constant of anandamide transfer from intracellular BSA complexes to the membrane outer leaflet (k_i) (Fig. 1) were found to vary with the $[BSA]_i$ such that k_i decreased with increasing $[BSA]_i$ (19). Because the rate constant of translocation (k_3) is constant for all $[BSA]$, it is apparent that the dissociation rate constant k_1 of anandamide-BSA complexes does not account for the fractional anandamide release to the water phase inside ghosts. This is because the ghost volume is unstirred; therefore, it is the effective mean dissociation constant, k_1^* , that is responsible for the anandamide release from BSA inside ghosts. In previous publications, a detailed account of the effects of an unstirred intracellular compartment is given (33, 34). The effective mean dissociation rate constant k_1^* is calculated from k_1 according to the equation $k_1^* = k_1 \frac{3}{r\lambda} \frac{\text{ctnh}(\lambda r) - 1}{(r\lambda)^2}$ [Appendix 3 equation A12 in Bojesen and Bojesen (34)], where r ($3 \text{ } \mu\text{m}$) is the radius of ghost (see Notations for λ). The calculated values of k_1^* are 0.92 ± 0.19 , 0.60 ± 0.10 , 0.44 ± 0.06 , and $0.29 \pm 0.04 \text{ s}^{-1}$ for $[BSA]_i$ of 7.5, 15, 30, and $60 \text{ } \mu\text{M}$, respectively.

DISCUSSION

The method we used here has previously been shown to be very successful for the elucidation of the mechanism by which ions and glucose pass the red blood cell membrane (27–29). Several temperatures were used in these studies, and they show that it is possible to investigate protein-mediated processes even at 0°C . However, the manual procedure does not allow temperatures $>0^\circ\text{C}$ in the cases

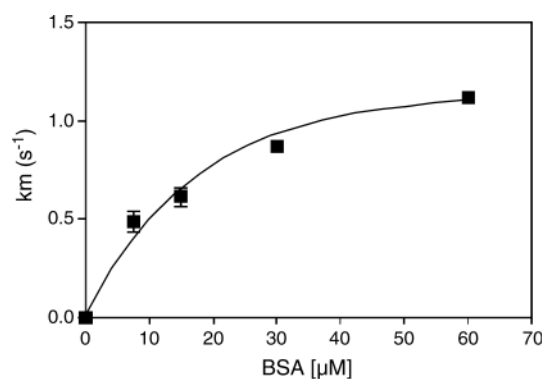


Fig. 3. Relationship between the rate constant (k_m) of unidirectional flow of [^3H]anandamide from the membrane outer binding pool (E) to BSA in the medium through the water phase and $[BSA]_o$. Error bars represent SD.

of fatty acids and anandamide, with the exception of oleic acid, which can be studied up to 20°C (I. N. Bojesen, unpublished data), because the transmembrane movements of these lipophilic molecules are so fast.

In the present system, the effect of the medium on the efflux kinetics of fatty acids was investigated previously (33–35). The data obtained could not be explained if the volume surrounding the ghosts was regarded as homogeneous with regard to tracer water phase concentration. Furthermore, we found that BSA of a limited volume was important (35). Likewise, a direct proportionality between the reciprocal constant $1/k_m$ (Fig. 1) (k_m , previously called k_5^*) and the reciprocal square root of BSA concentration outside the ghost cells ($[BSA]_o$) was found; in other words, k_m divided by the square root of $[BSA]_o$ was constant [(33) (Table 1)]. The same was found in the present study (Figs. 2B, 3), and this is a predicted effect if a UL is present (see Appendix for the theory).

Exchange efflux from BSA-free ghosts and BSA-filled ghosts

Strong evidence for the reliability of transport model I (Fig. 1) is seen in three findings: first, the ratio of anandamide bound to the inner membrane leaflet to anandamide bound to the outer membrane leaflet (B/E) and the rate constant of unidirectional flow through the membrane from B to E (k_3) are constants independent of $[BSA]_o$ (19); second, the rate constant of unidirectional flow from the ghost outer membrane leaflet (E) to BSA in the medium (k_m) strongly depends on $[BSA]_o$ (19) (Table 1), as mentioned above, such that $1/k_m$ is directly proportional to the reciprocal square root of $[BSA]_o$, as predicted by the effect of the UL as described in the Appendix; third, the experimental data fit to the theoretical data (see above).

In experiments with BSA-filled ghosts, the efflux kinetics is much slower than that in experiments with BSA-free ghosts. We found a decreasing effective mean dissociation rate constant of anandamide-BSA complexes (k_1^*) with increasing $[BSA]_i$. This effect of $[BSA]_i$ can be explained by a UL inside the ghosts. With an intracellular UL, we have a situation in which although BSA makes larger diffusional fluxes possible, it reduces the availability of unbound anandamide for uptake into the membrane phase.

Application of the results

In exchange efflux experiments, the net flux of radioactive anandamide is balanced by an equal and opposite movement of nonradioactive anandamide. This means that the k_m dependence of $[BSA]_o$ (Fig. 3) is also valid for uptake. Such dependence was previously observed in studies of fatty acid uptake into cells, in which fatty acids were offered to the cells bound to albumin (36, 37). The phenomenon shown in Fig. 3 was referred to as a “pseudo-facilitation mechanism” and explained by Weisiger, Pond, and Bass (30) as the existence of a disequilibrium layer within a UL. The concentration of unbound anandamide

is so low that a concentration gradient easily arises within the UL. This study, as well as our previous study on oleic acid (34), adds to an understanding of such dependence. The concentration of unbound anandamide is 7,000 times lower than that of anandamide bound to BSA. Therefore, the release of unbound anandamide from the membrane disturbs the local equilibrium between ligand and BSA. When $[BSA]$ is low, the possibility that an anandamide molecule can return to the membrane phase is highly likely, whereas this possibility becomes increasingly unlikely as the $[BSA]$ increases. In the situation of nonlimiting membrane permeability and with free anandamide concentration adjacent to the membrane lesser than the equilibrium concentration (P), the efflux rate [J (nmol s^{-1}); equal to the uptake rate] normalized to 1 ml (1 g) of ghosts can be calculated according to the equation

$$J = PCI_{\Sigma} = (K_d v S / (1 - v)) [D k_1 (1 - v) / K_d]^{1/2} [BSA]_o^{1/2} = \text{constant} [v / (1 - v)]^{1/2} \quad (\text{Eq. 17})$$

The values of K_d , S , and D are given in the Notations, $k_1 = 3.33 s^{-1}$, $60 \mu M$ (0.4%) is used for $[BSA]_o$, and v values are varied. **Figure 4** shows such uptake rate versus the water phase concentration of the free unbound anandamide [$P = K_d v / (1 - v)$; see Notations]. This plot obviously shows “saturation kinetics,” and if saturation kinetics is observed, it is not possible to distinguish between true saturation kinetics and a situation in which the membrane permeation is nonlimiting, and the uptake is determined by the clearance of unbound anandamide in the UL. The same form of curve is seen in studies of fatty acid efflux (34, 38) and in several studies of the short-term initial oleic acid uptake by metabolizing cells (39). Thus, taking the apparent saturation kinetics obtained for anandamide [for a critical review, see Glaser, Kaczocha, and Deutsch (20)] as a function of the total concentration, or even of the water phase concentration, as evidence for a membrane transporter may not be the correct

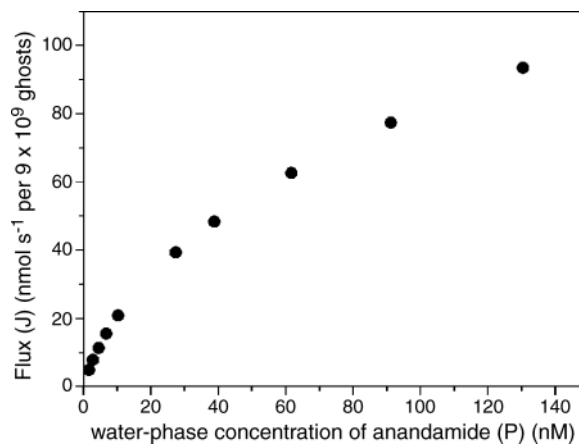


Fig. 4. Flux (J) dependence of the water phase concentration (P), illustrating that anandamide uptake is limited by permeation of a UL. J is calculated according to equation 17 at different v values and P as $K_d v / (1 - v)$ (see Notations). The values of $[BSA]_o$ and K_d are $60 \mu M$ and $6.87 nM$, respectively.

interpretation of the data, because such data could equally indicate a barrier function of the UL around the cells followed by a much faster membrane translocation.

The transport mechanism of anandamide has lately been much discussed, and evidence has been presented of a facilitated as well as of a simple diffusion (9, 11, 13, 17, 21, 22). The traditional indications for facilitated transport are *i)* saturation kinetics must occur; *ii)* a carrier protein must be present; *iii)* the protein must demonstrate a high degree of specificity; and *iv)* the protein must exhibit sensitivity to inhibition. Regarding indication *i)*, a saturable transport process is always taken as evidence for a facilitated transport involving a transport protein, but an apparent saturation kinetics might be a UL effect, as suggested by our findings here. It is important to realize that if permeability assays ignore the effect of UL, especially with lipophilic compounds, the resulting values will not correctly indicate the condition of transport but merely reveal a property of the water phase rather than of the membrane. Metabolism of anandamide by fatty acid amide hydrolase as well as binding to intracellular proteins may also contribute to saturation kinetics in studies of anandamide uptake into cells (10–12, 20). With regard to *ii)*, to our knowledge, a carrier protein has not been isolated and characterized, but it is known that anandamide can bind to ion channels or receptors in the membrane (40–44). As for points *iii)* and *iv)*, several inhibitors of anandamide receptors as well as of anandamide-hydrolyzing enzyme fatty acid amide hydrolase have been studied. These lipophilic anandamide analogs and inhibitors have been shown to influence the uptake rate (20, 25). Thus, anandamide uptake has been shown to be sensitive to several inhibitors when uptake is studied for time intervals of minutes (10–12, 20, 25), but the same inhibitors have no effects when anandamide uptake is investigated at early time points (17). These differences might be attributable to the incubation conditions. Transport inhibition studies carried out by Glaser, Kaczocha, and Deutsch (20) are always performed in the presence of BSA, whereas transport studies traditionally apply hydrophobic inhibitors dissolved in methanol, ethanol, or DMSO, with no protein present in the incubation medium. Such a procedure and incubation for minutes with high concentrations (micromolar) of lipophilic inhibitors may change the composition of the cellular membranes, with subsequent changes in anandamide uptake.

According to our previous study (19), anandamide membrane transport is extremely rapid. With 60 μM binding protein inside as well as outside the red blood cell ghosts, the half-life for transport through the membrane at 0°C to extracellular binding protein is ~ 16 s (19), so at 37°C, it is probably < 1 s. Therefore, the data obtained for uptake lasting for minutes are probably not valid for studying the pure transport process.

More serious is the fact already mentioned that experiments that form the basis for the postulate of a carrier protein mostly are carried out without albumin in the medium. In our experiments, no anandamide is released from the cells without protein in the medium. The molar

ratio of anandamide to albumin in body fluid is very low. With a plasma concentration of 4 nM, $> 99\%$ is bound to albumin (8). This means that anandamide in such experiments is offered to the cells in concentrations that exceed the monomer water phase concentration (8) by a factor of $> 10^6$. Anandamide is a hydrophobic compound and it adheres to glass tubes and plastic wells if not bound to albumin, so added to buffer directly or dissolved in alcohol, the actual concentration is unknown (18, 25).

As mentioned above, the membrane binding (M) has been used together with the inside/outside distribution (B/E) and the equilibrium dissociation constant (K_d) (19) to calculate the dissociation rate constant k_1 according to equation 8 at different corresponding k_m values and $[\text{BSA}]_o$ (Table 1). The calculation requires that the model is correct, but from the above discussion it seems reasonable to believe this. The value 3.33 s^{-1} is high compared with the dissociation rate constant for the long-chain fatty acids. The corresponding rate constant for arachidonic acid is 0.21 s^{-1} (45), and according to Demant, Richieri, and Kleinfeld (46), extrapolation of the arachidonic acid values to 0°C gives a constant of 0.67 s^{-1} . This means that the anandamide constant is 1 order of magnitude higher. This is surprising, but perhaps an explanation can be found by comparison with all of the fatty acids studied, with the exception of palmitic acid, that display diverging membrane binding characteristics ($B/E = 4\text{--}5$) (45, 47). Apparently, we have a linear relationship between changes in ΔG^* (activation free energy) and changes in ΔG^0 (reaction free energy). Thus, oleic acid as the most hydrophobic of the fatty acids has the highest binding constant K_a ($0.83 \times 10^9 \text{ M}^{-1}$) and the lowest dissociation rate constant k_1 (0.006 s^{-1}). The group of fatty acids with similar and lower hydrophobicity, arachidonic acid, linoleic acid, and docosahexaenoic acid (47), have lower binding constants (K_a values of 0.20, 0.28, and $0.24 \times 10^9 \text{ M}^{-1}$, respectively) and k_1 values 1 order of magnitude higher (0.21, 0.14, and 0.47 s^{-1}). Anandamide as the least hydrophobic compound has the lowest binding constant ($K_a = 0.14 \times 10^9 \text{ M}^{-1}$) and a k_1 of 3.33 s^{-1} , a value again 1 order of magnitude higher. This comparison makes sense, because we have shown that the carboxyl group does not contribute significantly to the free energy of binding of fatty acids to the hydrophobic channel in BSA by van der Waals-London dispersion interactions (48).

In conclusion, when highly hydrophobic compounds with fast transport across membranes are in question, the saturation kinetics seen in Fig. 4 may be understood as a $[\text{BSA}]$ dependence (i.e., as an effect of a rate-limiting delivery of anandamide from BSA in the UL).

APPENDIX

Notations

Δ : (μm) The thickness of the UL. The ghosts are in well-stirred suspensions surrounded by a UL, which in effect is a plane sheet, 6 μm deep and with the same area as a ghost (35).

- S: (μm^2) Surface area of ghosts normalized to 1 ml of ghosts containing 9×10^9 ghosts ($144 \times 9 \times 10^9 \mu\text{m}^2$).
- λ : (μm^{-1}) The length constant for transport in UL ($\ln 2/\lambda$ is the half length, where the concentration in the UL is half of the feeding concentration). It is defined as $(k_1 A/(P D))^{1/2} = [k_1 [\text{BSA}]_i(1 - \nu)/(K_d D)]^{1/2}$ (35). λ is calculated to 3.73, 5.27, 7.45, and $10.54 \mu\text{m}^{-1}$ for $[\text{BSA}]_i = 7.5, 15, 30,$ and $60 \mu\text{M}$, respectively. λ^{-1} represents a disequilibrium layer near the membrane surface, which decreases with increasing $[\text{BSA}]$ (30).
- V_u : (ml) Unstirred volume around ghosts equal to $\Delta \times S = 6 \times 144 \times 9 \times 10^9 \times 10^{-12} \text{ ml} = 7.8 \text{ ml}$.
- V_s : (ml) Stirred volume, $35 - 7.8 = 27.2 \text{ ml}$.
- V_0 : (ml) Total medium volume (35 ml).
- D: ($\mu\text{m}^2 \text{ s}^{-1}$) Diffusion coefficient of anandamide at 0°C (unknown). Calculated to $209.5 \mu\text{m}^2 \text{ s}^{-1}$.
- R_D : (s ml^{-1}) Diffusion resistance in the unstirred volume, equal to $\Delta/(S D) = 6/(144 \times 9 \times 10^9 \times 10^{-12} \times D)$. Calculated to 0.022 s ml^{-1} .
- k_1 : (s^{-1}) Dissociation rate constant of the anandamide-BSA complex.
- k_m : (s^{-1}) Rate constant of unidirectional flow from the ghost membrane to BSA in the medium through the water phase.
- k_5 : (s^{-1}) Rate constant of unidirectional flow from the ghost membrane to the adjacent water phase.
- k_3 : (s^{-1}) Rate constant of unidirectional flow through the membrane from B to E.
- y: (dpm) The amount of [^3H]anandamide in the medium at time t.
- y/y_∞ : The ratio of the amount of [^3H]anandamide in the medium at time t to that at infinite time.
- K_d : (M) Equilibrium dissociation constant at 0°C of anandamide binding to BSA, calculated for one binding site equal to 6.87 nM (8).
- M: (M) Concentration of anandamide bound to ghost membranes (19). $1 \text{ g ghost} = 1 \text{ ml}$.
- m: (dpm ml^{-1}) Concentration of [^3H]anandamide bound to ghost membranes.
- P: (M) Equilibrium water phase concentration of anandamide with one binding site on BSA, equal to $K_d \nu/(1 - \nu)$ (8).
- c_o : (dpm ml^{-1}) Water phase concentration of unbound [^3H]anandamide just outside the membrane.
- c_δ : (dpm ml^{-1}) Water phase concentration of unbound [^3H]anandamide everywhere in the stirred volume V_s .
- a: (dpm ml^{-1}) Concentration of [^3H]anandamide bound to BSA.
- A: (M) Concentration of anandamide bound to BSA.
- $[\text{BSA}]$: (M) Concentration of BSA in both V_u and V_s .
- ν : Molar ratio of anandamide to BSA equal to $A/[\text{BSA}]$.
- Cl_u : (s^{-1}) Clearance of V_u normalized to 1 ml of ghost cleared per second as a result of the concentration difference ($c_o - aP/A$) by binding to BSA in V_u , equal to $S(1 - e^{-\lambda\delta}) [[\text{BSA}] D(1 - \nu) k_1/K_d]^{1/2}$.

Cl_s : (s^{-1}) Clearance of V_s normalized to 1 ml of ghost cleared per second as a result of the concentration difference ($c_\delta - aP/A$) by binding to BSA in V_s , equal to $V_s k_1 [\text{BSA}] (1 - \nu)/K_d$.

Cl_Σ : (s^{-1}) Clearance of both volumes V_u and V_s , analogous to conductivity, equal to the sum Cl_u and $1/(1/\text{Cl}_s + R_D)$ (35).

B/E: Ratio of anandamide bound to the intracellular side of ghost membrane to anandamide bound to the extracellular side of ghost membrane.

Significance of the UL around ghosts

To understand the effect of $[\text{BSA}]$ on the rate constant, we have to consider the tracer uptake by BSA in the unstirred volume (V_u) as well as in the stirred volume (V_s). Anandamide is poorly soluble in water; therefore, it is impossible to dissolve anandamide in pure buffer and produce solutions with a well-defined monomer concentration of anandamide. However, in equilibrium with albumin-bound anandamide, a well-defined concentration can be obtained in buffer solutions at low ratios of anandamide to albumin. The water phase concentration of anandamide is low. With a high rate of uptake or release, small gradients can occur, which in the presence of a UL around the ghosts will influence the maximum uptake or release considerably. Thus, it is the binding to albumin that results in the efflux. For terms, see Notations.

The quasistationary efflux of tracer is based upon the principle of independent diffusion streams advocated by Jacobs (49). As described by Bojesen and Bojesen (35), the total flow of anandamide [$(F_1 + F_2)$, corresponding to the net uptake of tracer in V_u and V_s , respectively] can be expressed in terms of clearance. Thus

$$dy/dt = F_1 + F_2 \quad (\text{Eq. A1})$$

where

$$F_1 = \text{Cl}_u (c_o - aP/A) \quad (\text{Eq. A2})$$

$$F_2 = \text{Cl}_s (c_\delta - aP/A) \quad (\text{Eq. A3a})$$

$$F_2 = (1/R_D) (c_o - c_\delta) \quad (\text{Eq. A3b})$$

Eliminating c_δ from equations A3a and A3b gives

$$F_2 = [1/((1/\text{Cl}_s) + R_D)] (c_o - aP/A) \quad (\text{Eq. A4})$$

and thus

$$dy/dt = (c_o - aP/A) \text{Cl}_\Sigma \quad (\text{Eq. A5})$$

where $\text{Cl}_\Sigma = \text{Cl}_u + 1/((1/\text{Cl}_s) + R_D)$.

Furthermore, the flux between the membrane and medium space adjacent to the membrane is

$$dy/dt = k_5 M (m/M - c_o/P) \quad (\text{Eq. A6})$$

Elimination of c_o from equations A5 and A6 gives

$$dy/dt = k_5 m - k_5 M/P \text{Cl}_\Sigma [dy/dt + (aP/A) \text{Cl}_\Sigma] \quad (\text{Eq. A7})$$

and because $a = y/V_\theta$ and the tracer dose $T = m + y$, we get

$$dy/dt (1 + k_5 M / (P_{Cl_\Sigma})) = k_5 T - k_5 y - (k_5 M / (V_\theta A)) y \quad (Eq. A8)$$

or

$$dy/dt + [(k_5 P_{Cl_\Sigma} (V_\theta A + M)) / (V_\theta A (P_{Cl_\Sigma} + k_5 M))] y = [(k_5 P_{Cl_\Sigma}) / (P_{Cl_\Sigma} + k_5 M)] T$$

and because $V_\theta A \gg M$, we obtain the differential equation

$$dy/dt + [(k_5 P_{Cl_\Sigma}) / (P_{Cl_\Sigma} + k_5 M)] y = [(k_5 P_{Cl_\Sigma}) / (P_{Cl_\Sigma} + k_5 M)] T \quad (Eq. A9)$$

with the solution $y = T + C e^{-k_m t}$, where $k_m = (k_5 P_{Cl_\Sigma}) / (P_{Cl_\Sigma} + k_5 M)$.

For $t = 0, y = 0$, which means that $C = -T$, and for $t = \infty, y = y_\infty = T$. The solution is now $1 - y/y_\infty = e^{-k_m t}$ and

$$1/k_m = 1/k_5 + M / (P_{Cl_\Sigma}) \quad (Eq. A10)$$

Inserting $P = K_d v / (1 - v)$, $Cl_\Sigma = Cl_u + 1 / ((1/Cl_s) + R_D)$ and $Cl_u = S (1 - e^{-\lambda \delta}) (D (1 - v) (k_1 / K_d) [BSA])^{1/2}$ (35) in equation A10 yields

$$1/k_m = 1/k_5 + M(1 - v) / [v S (1 - e^{-\lambda \delta}) (D k_1 K_d (1 - v) [BSA])^{1/2} + K_d v / ((1/Cl_s) + R_D)] \quad (Eq. A11)$$

In this expression, $(1 - e^{-\lambda \delta}) \approx 1$ as λ is $(k_1 [BSA] (1 - v) / (K_d D))^{1/2}$, which means that for $\delta = 6 \mu\text{m}$, $e^{-\lambda \delta} = 2 \times 10^{-10}$ for $[BSA] = 7.5 \mu\text{M}$ and 3.5×10^{-28} for $[BSA] = 60 \mu\text{M}$.

We focus on the term $1 / ((1/Cl_s) + R_D)$. Cl_s is dependent on $[BSA]$, but the following considerations show that $1/Cl_s$ is negligible compared with R_D : *i)* $Cl_s = V_s k_1 [BSA] (1 - v) / K_d$; *ii)* $V_s = V_\theta - V_u = 35 - 7.8 = 27.2 \text{ ml}$ [see Notations and (35)].

With the values of the constant k_1 equal to 3.33 s^{-1} and K_d ($6.87 \times 10^{-12} \text{ mol ml}^{-1}$) published previously (8) and the experimental $v = 0.2$, $1/Cl_s$ varies from $1.3 \times 10^{-5} \text{ s ml}^{-1}$ at $[BSA] = 7.5 \times 10^{-9} \text{ mol ml}^{-1}$ to $1.6 \times 10^{-6} \text{ s ml}^{-1}$ at $[BSA] = 60 \times 10^{-9} \text{ mol ml}^{-1}$. These values are to be compared with R_D values of $2.2 \times 10^{-2} \text{ s ml}^{-1}$ (see Notations).

With $1/Cl_s \ll R_D$, we get

$$1/k_m = 1/k_5 + [M(1 - v) R_D / (K_d v)] / [R_D S (D k_1 (1 - v) / K_d)^{1/2} ([BSA])^{1/2} + 1] \quad (Eq. A12)$$

or

$$1/k_m = \text{constant 1} + \text{constant 2} [1 / (\text{constant 3} ([BSA])^{1/2} + 1)] \quad (Eq. A13)$$

where constant 1 = $1/k_5$, constant 2 = $M(1 - v) R_D / (K_d v)$, and constant 3 = $R_D S (D k_1 (1 - v) / K_d)^{1/2}$. This equation has been used to fit the three constants and show the k_m dependence of $[BSA]$.

If we choose to ignore completely the term $1 / ((1/Cl_s) + R_D)$ in Cl_Σ and the term $(1 - e^{-\lambda \delta})$, equation A10 reduces to


$$1/k_m = 1/k_5 + [M (1 - v)^{1/2} / (v S (D k_1 K_d)^{1/2})] 1 / ([BSA])^{1/2} \quad (Eq. A14)$$

or

$$1/k_m = 1/k_5 + \text{constant 4} (1 / ([BSA])^{1/2}) \quad (Eq. A15)$$

where

$$\text{constant 4} = M (1 - v)^{1/2} / (v S (D k_1 K_d)^{1/2}) \quad (Eq. A16)$$

Such a modification is reasonable because Cl_u is the dominant part of Cl_Σ . At $[BSA] = 7.5 \mu\text{M}$, we make an error of 4.5%, and at the higher $[BSA]$ of $60 \mu\text{M}$, the error is 1.6%. 

This study was supported by grants from the Novo Nordisk Foundation and the Carlsberg Foundation. Assistant Professor Niels Bindslev contributed important comments on the manuscript, and Aase Frederiksen provided skillful technical assistance. Both contributions are gratefully acknowledged.

REFERENCES

- Hansen, H. S., B. Moesgaard, H. H. Hansen, and G. Petersen. 2000. N-Acylethanolamines and precursor phospholipids—relation to cell injury. *Chem. Phys. Lipids*. **108**: 135–150.
- Hansen, H. H., P. C. Schmid, P. Bittigau, I. Lastres-Becker, F. Berrendero, J. Manzanares, C. Ikonomidou, H. H. O. Schmid, J. J. Fernández-Ruiz, and H. S. Hansen. 2001. Anandamide, but not 2-arachidonoylglycerol, accumulates during *in vivo* neurodegeneration. *J. Neurochem*. **78**: 1415–1427.
- Petersen, G., B. Moesgaard, P. C. Schmid, H. H. O. Schmid, H. Broholm, M. Kosteljanetz, and H. S. Hansen. 2005. Endocannabinoid metabolism in human glioblastomas and meningiomas compared to human non-tumor brain tissue. *J. Neurochem*. **93**: 299–309.
- Devane, W. A., L. Hanus, A. Breuer, R. G. Pertwee, L. A. Stevenson, G. Griffin, D. Gibson, A. Mandelbaum, A. Etinger, and R. Mechoulam. 1992. Isolation and structure of a brain constituent that binds to the cannabinoid receptor. *Science*. **258**: 1946–1949.
- Cravatt, B. F., K. Demarest, M. P. Patricelli, M. H. Bracey, D. K. Giang, B. R. Martin, and A. H. Lichtman. 2001. Supersensitivity to anandamide and enhanced endogenous cannabinoid signaling in mice lacking fatty acid amide hydrolase. *Proc. Natl. Acad. Sci. USA*. **98**: 9371–9376.
- Alger, B. E. 2004. Endocannabinoids: getting the message across. *Proc. Natl. Acad. Sci. USA*. **101**: 8512–8513.
- Hyde, R., P. M. Taylor, and H. S. Hundal. 2003. Amino acid transporters: roles in amino acid sensing and signalling in animal cells. *Biochem. J*. **373**: 1–18.
- Bojesen, I. N., and H. S. Hansen. 2003. Binding of anandamide to bovine serum albumin. *J. Lipid Res*. **44**: 1790–1794.
- Di Marzo, V., A. Fontana, H. Cadas, S. Schinelli, G. Cimino, J.-C. Schwartz, and D. Piomelli. 1994. Formation and inactivation of endogenous cannabinoid anandamide in central neurons. *Nature*. **372**: 686–691.
- McFarland, M. J., and E. L. Barker. 2004. Anandamide transport. *Pharmacol. Ther*. **104**: 117–135.
- Hillard, C. J., and A. Jarrahian. 2003. Cellular accumulation of anandamide: consensus and controversy. *Br. J. Pharmacol*. **140**: 802–808.
- Fowler, C. J., and S. O. Jacobsson. 2002. Cellular transport of anandamide, 2-arachidonoylglycerol and palmitoylethanolamide—targets for drug development? *Prostaglandins Leukot. Essent. Fatty Acids*. **66**: 193–200.

13. Fegley, D., S. Kathuria, R. Mercier, C. Li, A. Goutopoulos, A. Makriyannis, and D. Piomelli. 2004. Anandamide transport is independent of fatty-acid amide hydrolase activity and is blocked by the hydrolysis-resistant inhibitor AM1172. *Proc. Natl. Acad. Sci. USA*. **101**: 8756–8761.
14. Maccarrone, M., M. Bari, T. Lorenzon, T. Bisogno, V. Di Marzo, and A. Finazzi-Agrò. 2000. Anandamide uptake by human endothelial cells and its regulation by nitric oxide. *J. Biol. Chem.* **275**: 13484–13492.
15. Deutsch, D. G., S. T. Glaser, J. M. Howell, J. S. Kunz, R. A. Puffenbarger, C. J. Hillard, and N. Abumrad. 2001. The cellular uptake of anandamide is coupled to its breakdown by fatty-acid amide hydrolase. *J. Biol. Chem.* **276**: 6967–6973.
16. Fasia, L., V. Karava, and A. Siafaka-Kapadai. 2003. Uptake and metabolism of [³H]anandamide by rabbit platelets—lack of transporter? *Eur. J. Biochem.* **270**: 3498–3506.
17. Glaser, S. T., N. A. Abumrad, F. Fatade, M. Kaczocha, K. M. Studholme, and D. G. Deutsch. 2003. Evidence against the presence of an anandamide transporter. *Proc. Natl. Acad. Sci. USA*. **100**: 4269–4274.
18. Ortega-Gutiérrez, S., E. G. Hawkins, A. Viso, M. L. Lopez-Rodriguez, and B. F. Cravatt. 2004. Comparison of anandamide transport in FAAH wild-type and knock out neurons: evidence for contributions by both FAAH and CB1 receptor to anandamide uptake. *Biochemistry*. **43**: 8184–8190.
19. Bojesen, I. N., and H. S. Hansen. 2005. Membrane transport of anandamide through resealed human red cell membranes. *J. Lipid Res.* **46**: 1652–1659.
20. Glaser, S. T., M. Kaczocha, and D. G. Deutsch. 2005. Anandamide transport: a critical review. *Life Sci.* **77**: 1588–1604.
21. Sandberg, A., and C. J. Fowler. 2005. Measurement of saturable and non-saturable components of anandamide uptake into P19 carcinoma cells in the presence of fatty acid-free bovine serum albumin. *Chem. Phys. Lipids*. **134**: 131–139.
22. Ligresti, A., E. Morera, M. Van der Stelt, K. Monory, B. Lutz, G. Ortart, and V. Di Marzo. 2004. Further evidence for the existence of a specific process for the membrane transport of anandamide. *Biochem. J.* **380**: 265–272.
23. Avdeef, A. 2001. Physicochemical profiling (solubility, permeability and charge state). *Curr. Top. Med. Chem.* **1**: 277–351.
24. Naruhashi, K., I. Tamai, Q. Li, Y. Sai, and A. Tsuji. 2003. Experimental demonstration of the unstirred water layer effect on drug transport in Caco-2 cells. *J. Pharm. Sci.* **92**: 1502–1508.
25. Fowler, C. J., G. Tiger, A. Ligresti, M. L. López-Rodriguez, and V. Di Marzo. 2004. Selective inhibition of anandamide cellular uptake versus enzymatic hydrolysis—a difficult issue to handle. *Eur. J. Pharmacol.* **492**: 1–11.
26. Karlsson, M., C. Pahlsson, and C. J. Fowler. 2004. Reversible, temperature-dependent, and AM404-inhibitable adsorption of anandamide to cell culture wells as a confounding factor in release experiments. *Eur. J. Pharm. Sci.* **22**: 181–189.
27. Dalmark, M., and J. O. Wieth. 1972. Temperature dependence of chloride, bromide, iodide, thiocyanate and salicylate transport in human red cells. *J. Physiol.* **224**: 583–610.
28. Brahm, J. 1983. Kinetics of glucose transport in human erythrocytes. *J. Physiol.* **339**: 339–354.
29. Gasbjerg, P. K., and J. Brahm. 1991. Glucose transport kinetics in human blood cells. *Biochim. Biophys. Acta.* **1062**: 83–93.
30. Weisiger, R. A., S. M. Pond, and L. Bass. 1989. Albumin enhances unidirectional fluxes of fatty acid across a lipid-water interface: theory and experiments. *Am. J. Physiol.* **257**: G904–G916.
31. Piomelli, D., A. Giuffrida, A. Calignano, and F. Rodriguez de Fonseca. 2000. The endocannabinoid system as a target for therapeutic drugs. *Trends Pharmacol. Sci.* **21**: 218–224.
32. Bojesen, I. N., and E. Bojesen. 1991. Palmitate binding to and efflux kinetics from human erythrocyte ghost. *Biochim. Biophys. Acta.* **1064**: 297–307.
33. Bojesen, I. N., and E. Bojesen. 1995. Arachidonic acid transfer across the human red cell membrane by a specific transport system. *Acta Physiol. Scand.* **154**: 253–267.
34. Bojesen, I. N., and E. Bojesen. 1996. Oleic acid binding and transport capacity of human red cell membrane. *Acta Physiol. Scand.* **156**: 501–516.
35. Bojesen, I. N., and E. Bojesen. 1992. Exchange efflux of [³H]palmitate from human red cell ghosts to bovine serum albumin in buffer. Effects of medium volume and concentration of bovine serum albumin. *Biochim. Biophys. Acta.* **1111**: 185–196.
36. Sorrentino, D., K. Van Ness, and P. D. Berk. 1994. Oleate uptake kinetics in the perfused rat liver are consistent with pseudofacilitation by albumin. *J. Hepatol.* **21**: 551–559.
37. Weisiger, R., J. Gollan, and R. Ockner. 1981. Receptor for albumin on the liver surface may mediate uptake of fatty acids and other albumin-bound substances. *Science.* **211**: 1048–1051.
38. Bojesen, I. N., and E. Bojesen. 1992. Water-phase palmitate concentrations in equilibrium with albumin-bound palmitate in a biological system. *J. Lipid Res.* **33**: 1327–1334.
39. Sorrentino, D., R. B. Robinson, C. L. Kiang, and P. D. Berk. 1989. At physiologic albumin/oleate concentrations oleate uptake by isolated hepatocytes, cardiac myocytes, and adipocytes is a saturable function of the unbound oleate concentration. Uptake kinetics are consistent with the conventional theory. *J. Clin. Invest.* **84**: 1325–1333.
40. Johnson, D. E., S. L. Heald, R. D. Dally, and R. A. Janis. 1993. Isolation, identification and synthesis of an endogenous arachidonic amide that inhibits calcium channel antagonist 1,4-dihydropyridine binding. *Prostaglandins Leukot. Essent. Fatty Acids.* **48**: 429–437.
41. Oliver, D., C.-C. Lien, M. Soom, T. Baukowitz, P. Jonas, and B. Fakler. 2004. Functional conversion between A-type and delayed rectifier K⁺ channels by membrane lipids. *Science.* **304**: 265–270.
42. Maingret, F., A. J. Patel, M. Lazdunski, and E. Honoré. 2001. The endocannabinoid anandamide is a direct and selective blocker of the background K⁺ channel TASK-1. *EMBO J.* **20**: 47–54.
43. Di Marzo, V., L. De Petrocellis, F. Fezza, A. Ligresti, and T. Bisogno. 2002. Anandamide receptors. *Prostaglandins Leukot. Essent. Fatty Acids.* **66**: 377–391.
44. Lozovaya, N., N. Yatsenko, A. Beketov, T. Tsintsadze, and N. Burnashev. 2005. Glycine receptors in CNS neurons as a target for nonretrograde action of cannabinoids. *J. Neurosci.* **25**: 7499–7506.
45. Bojesen, I. N., and E. Bojesen. 1998. Nature of the elements transporting long-chain fatty acids through the red cell membrane. *J. Membr. Biol.* **163**: 169–181.
46. Demant, E. J. F., G. V. Richieri, and A. M. Kleinfeld. 2002. Stopped-flow kinetic analysis of long-chain fatty acid dissociation from bovine serum albumin. *Biochem. J.* **363**: 809–815.
47. Bojesen, I. N. 2002. Studies of membrane transport mechanism of long-chain fatty acids in human erythrocytes. In *Recent Research in Development of Membrane Biology*. S. G. Pandalai, editor. Research Signpost, Trivandrum, India. **1**: 33–50.
48. Bojesen, I. N., and E. Bojesen. 1996. Albumin binding of long-chain fatty acids: thermodynamics and kinetics. *J. Phys. Chem. B.* **100**: 17981–17985.
49. Jacobs, M. H. 1967. *Diffusion Processes*. Springer, Berlin.